A New Method to Improve Multibiometric Recognition

Rodolfo Vertamatti & Miguel Arjona Ramirez

***Abstract*— Multibiometrics has several advantages over single biometric analysis. However, if all traits are almost identical, as for twins, multiple source processing does not improve performance. To overcome extreme similitude, genetic code is not as important as epigenetic and environmental influences. This study examines phenotypic plasticity in human asymmetry as a tool to ameliorate multibiometrics. A technique called Bilateral Processing (BP) is described here to analyze discordances in left and right trait sides by using Cross-Correlation, Wavelets and Neural Networks in visible and infrared spectrum images. Used traits were teeth, ears, irises, fingerprints, noses and cheeks. Acoustic BP was also implemented for vibration asymmetry evaluation during vocal sounds and compared to MFCC plus Vector Quantization speaker recognition. Image and acoustic BP assessed nine brothers during one year. For test purposes, left biometrics was impostor to right biometrics from the same individual and vice-versa. Results achieved better performance in all biometrics treated with BP than without BP.**

***Index Terms*— Biometrics, Human Fluctuating Asymmetry, Multibiometrics.**

***Resumo*—Este documento contém informações para a preparação da versão final de um artigo aceito para publicação na Revista Telecomunicações. Por favor siga cuidadosamente as instruções para garantir a legibilidade e uniformidade dos artigos aceitos.**

***Palavras chave*—Aproximadamente quatro palavras chave ou frases em ordem alfabética, separadas por vírgulas.**

I. Introduction

Ensemble of biometric sources using proper fusion methods outperforms each of the individual source performances. Besides, noise and impostor attacks can be circumvented by the use of multi-sensor, multi-modal biometrics [1].

Notwithstanding, multibiometrics becomes useless when distinguishing extreme biometric similarities, as for monozygotic twins (MZ). Results tend to mistake twins and extra traits do not raise separability. To solve this, biometrics should consider human features in which DNA is not the determining factor in order to overcome limits imposed by narrow genetic distance.

Human bilateral trait sides (BL) are composed of two quasi-identical enantiomorphic images (left and right). Despite pertaining to the same person, if one of the sides is horizontally reflected, one can look for BL idiosyncrasies.

Manuscrito recebido em 15 de maio de 2011; revisado em 21 de novembro de 2011.

R. Vertamatti (rvertama@usp.br) and M. A. Ramírez (miguel@lps.usp.br) are from Signal Processing Laboratory, Escola Politécnica – University of São Paulo. Av. Prof Luciano Gualberto, trav. 3, 158. 05508-970, São Paulo-SP, Brazil.

With proper resolution, each human trait is one-of-a-kind – including BL of a person – as observed in ears [2], irises [3], fingerprints [4], etc. Differences in equal DNA entities (like BL) are caused by epigenetic or environment influences.

This study presents the implementation aspects of a new technique called Bilateral Processing (BP) that stresses left vs. right peculiarities. The paper is an extended version of [5] by adding implementation decisions and mathematical descriptions of algorithms. To test BP concept, a comprehensive approach is necessary, i.e., including multiple sensors, algorithms, classifications, and instances. Seven biometric traits, captured by three sensors, are tested in three recognition systems. BP is compared to "without BP" systems under the same circumstances. Implementation structure is presented in section II, along with the results obtained.

II. Bilateral Processing Implementation

Figure 1 exhibits several biometric traits from MZ twins: face, teeth, eyes and palms. Chirality is removed from the left sides traits, so left and right sides can be compared directly. From the comparison, one can observe that any permanent left and right discrepancy is potentially capable of differentiating MZ. Permanent fluctuating asymmetry can be caused by epigenetic influences, e.g., naevi, or environment influences, e.g., broken tooth, and as independent from genetic code, it is random and specific for each human being.

The search for left-right idiosyncrasies in biometric traits is the essence of the Bilateral Processing technique. BP compensates misalignments and segregates asymmetrical from symmetrical parts. Misalignments are biometric information, but their compensation is required in top-down focus on subtle details, e.g., texture. Segregation reduces dimensionality, by emphasizing on differences and disregarding similarities.

Figure 2 shows the block diagram of the recognition system divided into sensors, pre-processing, BP, classification and fusion during database formation (training) and testing.

BP is composed of alignment, segmentation and bilaterism. In alignment, samples are centralized by trait-specific reference marks. Segmentation divides the trait in potential biometric areas. Bilaterism outputs a list of asymmetric segments. This list is used during the test phase to localize singularities. Table I summarizes the conditions to test BP. Traits, sensors, test conditions, algorithm and results are described in the following sections.

TABLE I

RATIONALE FOR BILATERAL PROCESSING TESTS

Item	Characteristics	Reason
Population	Nine male brothers	Brothers are the narrowest genetic distance, except monozygotic twins.
Acquisition	One year and up to 20 samples per person	Time and quantity of samples enough to check biometric trait stability.
Environment	Personal Computer	Flexibility and availability. Routines run in PC Duo CPU E6550, 2,3GHz e 2G RAM.
BL x BL	Opposite BL as impostor	If chirality is reversed, BL differentiation is difficult task, even for the owner of the biometric characteristic, unless prominent.
BP x without BP	Technique confrontation	Comparative test to check BP technique efficiency. Under the same conditions, like similar sample data file sizes, how each technique performs.
Sensor 1	Visible spectrum camera	High-resolution camera and high magnification lens to emphasize subtle asymmetries in biometric traits.
Sensor 2	Infrared spectrum camera	Thermal emission to assert asymmetries in internal vascular system below face skin. Internal organs tend to be more asymmetrical than the visible ones.
Sensor 3	Pair of contact microphones	Asymmetrical Face reverberation during pronunciation. Ambient wall reflections are considered negligible.
Image Method 1	Correlation Pattern Recognition (CPR)	CPR is a method without intermediary parameterization and classification is via complete comparison test versus database.
Image Method 2	Wavelet + NN	Method using wavelet parameterization for space and frequency separation and non-linear Neural Network classification.
BP Acoustic Method	Pan	Normalized left-right differences to detect epidermal reverberation, by the use of panning audio functions.
Without BP Acoustic Method	MFCC + VQ	Without BP method is an extra and not derived from BP method, due to inherent bilateral difference in BP, which does not present the audio channels independently.
Biometric trait 1 captured by visible spectrum sensor	Tooth	Frontal teeth stability and easy accessibility are the main reasons for biometric choice. To obtain the complete dental arch is ideal but highly intrusive.
Biometric trait 2 captured by visible spectrum sensor	Ear	Ear cartilage contour and ear veins format are stable in time. Ear occlusions by hair should be avoided.
Biometric trait 3 captured by visible spectrum sensor	Nostril	Nasal cartilage is stable, except during exacerbated respiration due to nostril dilation. Nostrils are photographed from below.
Biometric trait 4 captured by visible spectrum sensor	Fingerprint	Centralized at the main whorl / loop / arch of the index finger. The non-contact acquisition is at fingerprint pore resolution.
Biometric trait 5 captured by visible spectrum sensor	Iris	Inferior iris hemisphere is used to avoid the common lid and eyelashes occlusion and flash reflections that occur at the superior iris hemisphere.
Biometric trait captured by infrared spectrum sensor	Cheek	This face region is used to avoid geographic coincidence with biometric traits captured by the visual spectrum sensor.
Biometric trait captured by acoustic sensor	Face vibration during vocalic sounds	Contact microphones positioned over the masseter muscle, which coincides with a highly vibrational face region.

A. Biometric Traits in accordance to Sensors

1) Visible Spectrum Images:

Images taken in the 0.39 μm to 0.75 μm wavelength region. Selected traits are: teeth shape, ears veins and contours, irises pattern, fingerprints ridges and nostrils formats.

2) Infrared Spectrum Images:

Images taken in the 8 μm to 13 μm spectrum range. Human thermal emission peaks around 9.5 μm. Infrared images indicate internal vascular system and organ activities. This study monitored facial cheeks inequalities.

3) Skin Vibration during Vocalic Sounds:

Several kinds of acoustic waves (longitudinal, transverse, surface, etc) propagate inside the body during voiced sounds. As consequence, complex vibrational modes appear on the skin surface. Due to body asymmetry, vibrational modes are asymmetric as well. Sensors positioned in symmetrical areas measure left and right facial vibrations during constant pitch diphthong ("a" + "i") phonation.

B. Sensors

1) Visible spectrum sensor:

A full-frame sensor is used with 21.1 Mpixels and radiometric resolution of 14-bit per red, green and blue channels. Lens has f/2.8 of maximum aperture, f/16 of minimum aperture and magnification from 1 to 5 times.

2) Infrared sensor:

Uncooled focal plane array microbolometer with 19.2 kpixel, ±0.1°C of precision, ±2ºC of accuracy and 3.1mrad of instantaneous field of view.

3) Acoustic sensor:

Two capacitive contact microphones symmetrically located on left and right masseter muscles. The sampling rate to both channels is 48 kHz and 16384-sample window is used to detect low-frequency variations (below 15 Hz).

C. Test Conditions

The test population is composed of nine adult male brothers (brothers have the lowest genetic distance with the exception of twins). Up to 20 samples per trait are taken over one year. For test purposes, right biometric trait is impostor to the left one (with chirality reversal) and vice-versa. BL of 9-person population turns into 18x18 identification matrix per biometric trait. With these conditions, the total amount of acquisition sessions surpasses 2000 sessions for the whole population.

D. Specific Bilateral Processing

Two image BP (Correlation and Wavelet + NN) and one acoustic BP were implemented. Both image BPs processed visible and infrared spectrum images. Alignment means left-right image registration. Acoustic BP does not require alignment due to fact that left and right channels are recorded simultaneously. Segmentation is the decomposition of the bio-signal: for images is fragmentation into smaller rectangles, whereas for acoustic signals it is the separation of the main harmonics of voiced sounds. Bilaterism compares left and right segments. No execution of segmentation and bilaterism characterizes the image non-BP, and whole trait images are used instead of segments. Whole trait and segments are formatted to equivalent image sizes. The three methods are described next along the figures 3 to 6.

1) Image Method 1: Correlation Pattern Recognition

CPR has extensive applications in pattern classification. CPR advantages are integrative operation and shift-invariant. However, it is overly sensitive to noise and rotation [6].

To determine what pair of bilateral segments are relevant, BP method 1 uses normalized cross-correlation on each pair of right (*r*) and left (*l*) segments as follows:

$$\beta(u,v)=\frac{\sum_{x,y}\left[r(x,y)-\bar{r}\right]\left[l(x-u,y-v)-\bar{l}\right]}{\sqrt{\sum_{x,y}\left[r(x,y)-\bar{r}\right]^2\sum_{x,y}\left[l(x-u,y-v)-\bar{l}\right]^2}} \quad (1)$$

where $\bar{r}$ and $\bar{l}$ are segment averages; *x,u,y,v* are image indices. β_{PEAK} is the maximum value of $\beta(u,v)$. Positions of the 5 most asymmetric segment pairs (the five lowest β_{PEAK}) are saved.

When the list of most dissymmetrical pairs of segments is determined, the system is ready to compare the test segment (*t*) to the database (*b*) by using the same normalized cross-correlation equation:

$$\gamma(u,v)=\frac{\sum_{x,y}\left[t(x,y)-\bar{t}\right]\left[b(x-u,y-v)-\bar{b}\right]}{\sqrt{\sum_{x,y}\left[t(x,y)-\bar{t}\right]^2\sum_{x,y}\left[b(x-u,y-v)-\bar{b}\right]^2}} \quad (2)$$

where $\bar{t}$ and $\bar{b}$ are segment averages. γ_{PEAK} is the maximum value of $\gamma(u,v)$. The test segment with the highest correlation γ_{PEAK} determines the identification match.

Figure 3 presents the matrix of γ_{PEAK} obtained by the Correlation Pattern Recognition method, exemplified by irises. Test samples and database are divided in two sets: "with BP" and "without BP". "With BP" uses 5 segments positions per person. "Without BP" uses the same equation (2), but instead of segments, the whole biometric trait is considered. The test sample is compared to the complete database.

2) Image Method 2: Wavelet + NN

Wavelet parameterization is a non-holistic approach with space and frequency separation. Bilateral images are subtracted one from another and emphasis can be put on specific parameters. Neural Network (NN) is a non-linear classification used in a complex environment of biometric fuzzy comparisons.

Wavelet parameterization [7] and Neural Network classification [8] method is illustrated on figure 4. Eighteen whole traits for non-BP and 810 segments (5 segment positions per person) for BP are transformed into wavelet coefficients and compared to the database via two-layers neural network.

Bidimensional wavelets can be obtained by the product of unidimensional scale (ϕ) and wavelet functions (ψ):

$$\phi(x,y)=\phi(x)\cdot\phi(y) \quad (3)$$

$$\psi^H(x,y) = \phi(x) \cdot \psi(y) \quad (4)$$

$$\psi^V(x,y) = \psi(x) \cdot \phi(y) \quad (5)$$

$$\psi^D(x,y) = \psi(x) \cdot \psi(y) \quad (6)$$

$\psi^H(x,y)$, $\psi^V(x,y)$ and $\psi^D(x,y)$ are respectively 2D horizontal, vertical and diagonal wavelet functions. The difference of left (l) and right (r) images can be seen on figure 5. The parameterization of $|l - r|$ are obtained by subtracting:

$$l = \sum_{\boldsymbol{k} \in \mathbf{Z}^2} a_{j_0,\boldsymbol{k}} \phi_{j_0,\boldsymbol{k}} + \sum_{\boldsymbol{k} \in \mathbf{Z}^2} b^{\lambda}_{j,\boldsymbol{k}} \psi^{\lambda}_{j,\boldsymbol{k}} \quad (7)$$

$$r = \sum_{\boldsymbol{k} \in \mathbf{Z}^2} c_{j_0,\boldsymbol{k}} \phi_{j_0,\boldsymbol{k}} + \sum_{\boldsymbol{k} \in \mathbf{Z}^2} d^{\lambda}_{j,\boldsymbol{k}} \psi^{\lambda}_{j,\boldsymbol{k}} \quad (8)$$

where $\lambda = H, V, D$ and :

$a_{j_0,k} = \langle l, \phi_{j_0,k} \rangle$, $b^{\lambda}_{j,k} = \langle l, \psi^{\lambda}_{j,k} \rangle$, $c_{j_0,k} = \langle r, \phi_{j_0,k} \rangle$, $d^{\lambda}_{j,k} = \langle r, \psi^{\lambda}_{j,k} \rangle$;

The dilated and translated functions $\{\psi^{\lambda}_{j,k}(x,y): j \in \mathbf{Z}; k \in \mathbf{Z}^2; \lambda = H, V, D\}$ and $\{\phi_{j,k}(x,y): j \in \mathbf{Z}; k \in \mathbf{Z}^2\}$ form orthonormal base $\mathbf{L^2(R^2)}$. The positions of the five segment pairs with the highest absolute value of wavelet subtraction are saved.

This five segment positions are used to classify by feed-forward two-layer perceptrons using supervised learning algorithm:

$$z_k = \sigma\left(\sum_{j=1}^{P} w^{(2)}_{kj} h\left(\sum_{i=1}^{S} w^{(1)}_{ji} f_i + w^{(1)}_{j0} \right) + w^{(2)}_{k0} \right); \quad (4)$$

where f are the S-size segment wavelet coefficients, P is the size of the hidden layer. $\sigma(.)$ and $h(.)$ are hyperbolic tangent sigmoid transfer functions. w are the weights – whose layers are superscripted. Training is optimized by gradient descent with adaptive learning backpropagation. "Without BP" uses the same algorithm, but instead of segments, the whole biometric trait is considered.

1) Acoustic Method

In the acoustic BP, the vocalic signal is segmented in each of the harmonics of the constant voice pitch:

$$L_H(e^{j\omega}) = F_H(e^{j\omega}) L(e^{j\omega}) = F_H(e^{j\omega}) \sum_{m=-\infty}^{\infty} l[m] \Lambda[n-m] e^{-j\omega m} = \Im(l_H) \quad (9)$$

$$R_H(e^{j\omega}) = F_H(e^{j\omega}) R(e^{j\omega}) = F_H(e^{j\omega}) \sum_{m=-\infty}^{\infty} r[m] \Lambda[n-m] e^{-j\omega m} = \Im(r_H) \quad (10)$$

where L and R are the FFT ($\Im(.)$) of the channels l and r respectively. Λ is 16384-sample Kaiser window. F_H is the band-pass filter for the Hth fundamental frequency harmonic. Similarly, filtered L_H and R_H are the FFT of l_H and r_H. As the voice signal is purely vocalic and of constant pitch ω_0:

$$l[m] = \sum_{H=1}^{\infty} l^A_H[m] \cos(H\omega_0 m + l^{\phi}_H) \quad (11)$$

$$r[m] = \sum_{H=1}^{\infty} r^A_H[m] \cos(H\omega_0 m + r^{\phi}_H) \quad (12)$$

where A and ϕ superscripts in l_H and r_H are the respective amplitude and phase. Normalized functions A_H and ϕ_H are the relative amplitude and phase between both channels per harmonic H, being $A_H \in [-1, +1]$ and $\phi_H \in [-\pi, +\pi]$. A_H and ϕ_H functions vary in time and they represent the asymmetric vibrational modes on the microphone contact area:

$$A_H = \frac{l^A_H - r^A_H}{l^A_H + r^A_H} \quad (13)$$

$$\phi_H = l^{\phi}_H - r^{\phi}_H \quad (14)$$

Figure 6 depicts an example: 4th harmonic is extracted from diphthong [ai] and left and right channels are confronted by a normalized difference equation, whose amplitude variation is shown. Phase and amplitude behavior of each harmonic are particular to each person and his/her left and right channels. Differently to the image BP, acoustic BP cannot be adapted as non-BP, thus a new speaker recognition system based on 20-triangular-filter MFCC [9] and 16-centroid Vector Quantization [10] was created to identify the 9 left and 9 right channels.

E. Results

The tables below show obtained results for "with BP" and "without BP", already presented in [11]. Table II exhibits the results of both image recognition methods. In both cases, bilateral processing substantially improved the performance. The acoustic data from table III indicates that non-BP identified persons, but confused their channel sides, while BP identified persons and left or right channel origin.

TABLE II
WITH AND WITHOUT IMAGE BILATERAL PROCESSING

Image Biometric Trait	Cross-Correlation: Minimum Genuine/Impostor Relation		Wavelet + Neural Networks	
	Without Bilateral Processing	With Bilateral Processing	Without Bilateral Processing	With Bilateral Processing
TOOTH	0,85	1,01	28%	100%
EAR	0,72	1,46	25%	100%
EYE	0,96	2,48	12%	100%
FINGER	0,88	1,48	30%	100%
NOSE	0,57	1,13	34%	100%
CHEEK	0,75	1,10	33%	100%

TABLE III
WITH AND WITHOUT ACOUSTIC BILATERAL PROCESSING

Acoustic Biometric Trait	Non-BP by MFCC and Vector Quantization		BP by normalized channel subtraction (18 channels)
	(9 persons)	(18 channels)	
VOICE	100%	44%	100%

III. CONCLUSIONS

Results show that Bilateral Processing was necessary to achieve maximum identification at segment level in small and low genetic distance population. Chosen segments proved stability over one year.

Few researches consider human asymmetry in biometrics. It is a field of great potential to extend analysis to larger population, different sensors and biometric traits. It brings double dimension to match decisions and intensifies epigenetic and environmental influences.

REFERENCES

[1] L. Hong, A. K. Jain and S. Pankanti, "Can multibiometrics improve performance?" in *Proc. IEEE Workshop on Automatic Identification Advanced Technologies*, New Jersey, 1999, pp 59–64.

[2] A. Iannarelli, *Ear Identification* (Forensic Identification Series). Fremont, Calif.: Paramount Publishing Company, 1989, preface.

[3] J. Daugman and C. Downing, "Epigenetic randomness, complexity and singularity of human iris patterns," *Proc. Royal Society*, vol. 268, pp. 1737–1740, 2001.

[4] A. K. Jain, S. Prabhakar and S. Pankanti, "On the similarity of identical twin fingerprints," *Pattern Recognition*, vol. 35, pp. 2653–2662, 2002.

[5] R. Vertamatti, M. Arjona Ramírez, "A new method to improve multibiometric recognition," in: *Int. Workshop on Telecommunications*, 2011, Rio de Janeiro. *Proceedings of the International Workshop on Telecommunications.* IWT 2011. Santa Rita do Sapucaí: Instituto Nacional de Telecomunicações, 2011, pp. 31–34.

[6] B. V. K. V. Kumar, A. Mahalanobis and R. D. Juday, *Correlation Pattern Recognition.* N. York: Cambridge Univ. Press, 2005, pp. 1–12.

[7] Y. Y. Tang, L. H. Yang, J. Liu and H. Ma, *Wavelet Theory and its Application to Pattern Recognition.* World Scientific, 2000, pp. 1–51.

[8] C. M. Bishop, *Neural Networks For Pattern Recognition.* Oxford, UK: Clarendon Press, 1995, pp. 116–163.

[9] T. Ganchev, N. Fakotakis, and G. Kokkinakis, "Comparative evaluation of various MFCC implementations on the speaker verification task," in *10th Int. Conf. on Speech and Computer*, 2005, vol. 1, pp. 191–194.

[10] Y. Linde, A. Buzo and R. M. Gray, "An algorithm for vector quantizer design," *IEEE Trans. Comm.*, vol. COM 28, pp. 84–95, Jan. 1980.

[11] R. Vertamatti, M. Arjona Ramírez, "Human asymmetry in multibiometric recognition," in: *IEEE Workshop on Computational Intelligence in Biometrics and Identity Management* CIBIM 2011, Session on "New and non-conventional Biomectrics: Algorithms, Methods and Systems", 2011, Paris. *Proc. of IEEE Workshop on Computational Intelligence in Biometrics and Identity Management.* CIBIM 2011. New Jersey: IEEE Press, pp. 70-77, 2011.

[12] D. Teplica and K. Peekna, "The mirror phenomenon in monozygotic twins", in *Multiple Pregnancy Epidemiology, Gestation & Perinatal Outcome*, I. Blickstein and L. G. Keith, Eds, 2nd ed. London: Informa, 2006, pp. 277–288.

[13] Casia Iris-Twins Database version 4.0 from Biometrics Ideal Test, http://biometrics.idealtest.org/downloadDB.do?id=4&subset=3.

[14] G. Lu, D. Zhang, W. K. Kong, and M. Wong, "A palmprint authentication system,"in *Handbook of Biometrics*, A. K. Jain, P. Flynn, A. A. Ross. (Eds.). New York: Springer, 2008, pp.185.

Rodolfo Vertamatti was born in São Bernardo do Campo, SP, Brazil. He has the following degrees: Electronic Technician (ETI Lauro Gomes, Brazil, 1979), Electronic Engineer (Instituto Tecnológico de Aeronáutica, Brazil, 1984), M.S. and Dr. in Electrical Engineering (University of São Paulo, 1989 and 2011).

From 1985 to 2002 he worked in Alcatel Company in Brazil and Europe for software and hardware development, design specification and product management of telecommunication equipments.

Since 2003 he is working in editing and publishing area. He is author of four books. His research interests are: audio, image and video digital processing, pattern recognition, and biometrics.

Miguel Arjona Ramírez is Associate Professor at Escola Politécnica, University of São Paulo, where he is a member of the Signal Processing Laboratory. He received the E.E. degree from Instituto Tecnológico de Aeronáutica, Brazil, and the M.S., the Dr. and the Habilitation (Livre-Docência) degrees in Electrical Engineering from University of São Paulo, Brazil, in 1992, 1997 and 2006, respectively, and the Electronic Design Eng. degree from Philips International Institute, The Netherlands, in 1981. In 2008 he carried post-doctoral research in time-frequency speech analysis and coding at the Royal Institute of Technology in Stockholm, Sweden.

He was Engineering Development Group Leader for Interactive Voice Response Systems (IVRs) for Itautec Informática, Brazil, where he served from 1982 to 1990. He is a Senior Member of the IEEE since 2000, a Member of the Brazilian Telecommunications Society (SBrT) and a Member of the IEICE. His research interests include signal compression, speech analysis, coding and recognition, and audio analysis and coding.

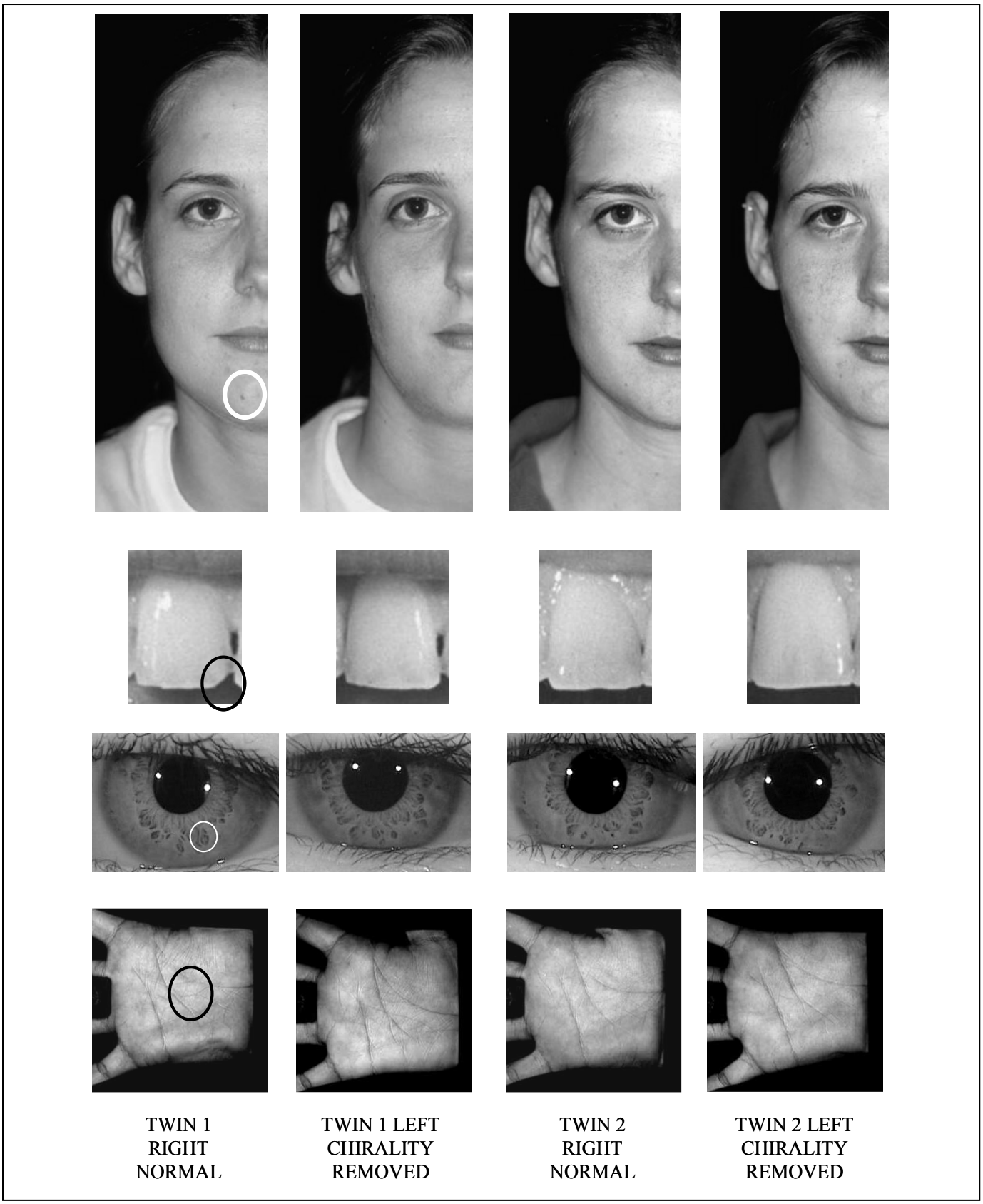

Fig. 1: Bilateral asymmetry tends to be monozygotic twin discrepancies as well. Photographs from MZ twins: face (D. Teplica [12]), teeth (Life Photo Archive), Iris (Casia-twin database [13]) and palmprints [14]. Twin left photos are horizontal or vertical reflections in order to remove chirality.

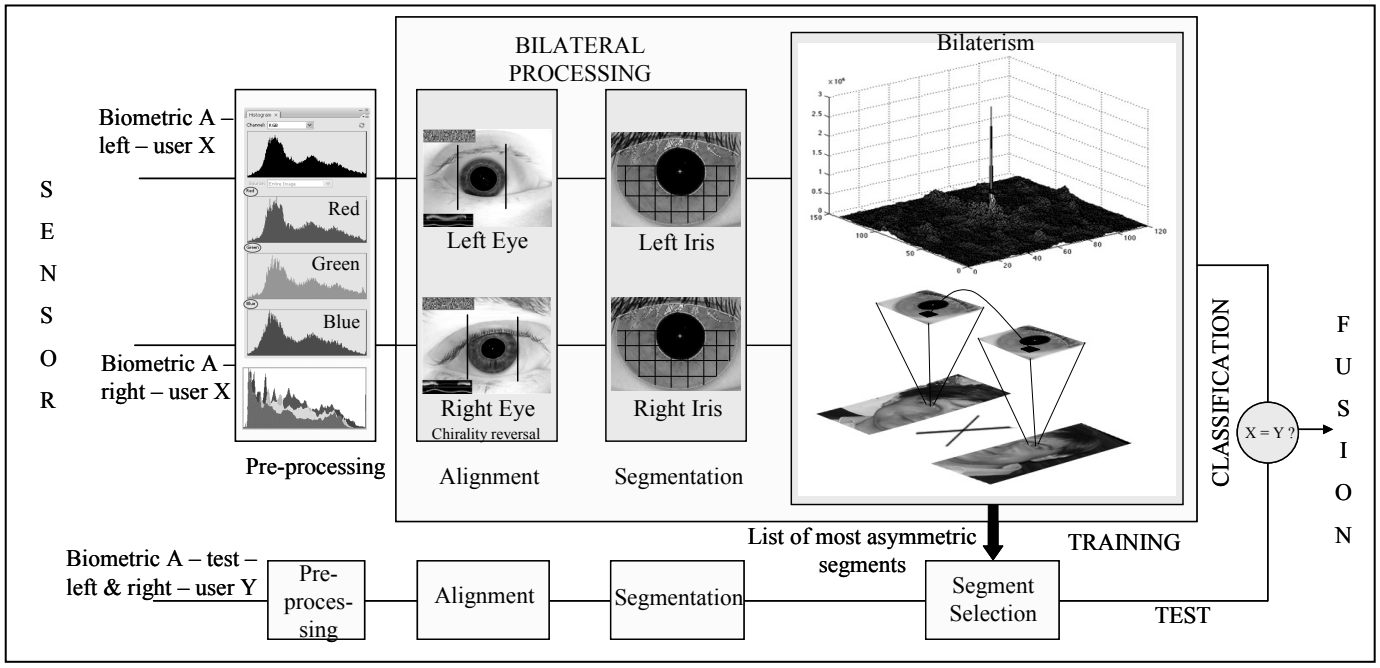

Fig. 2: Block Diagram of the Recognition system with Bilateral Processing (BP) incorporated. It is divided in training and test. Database access is implicit. Training, besides database formation, outputs a list of the positions of the most asymmetric segments. This list is used to select segments to be classified.

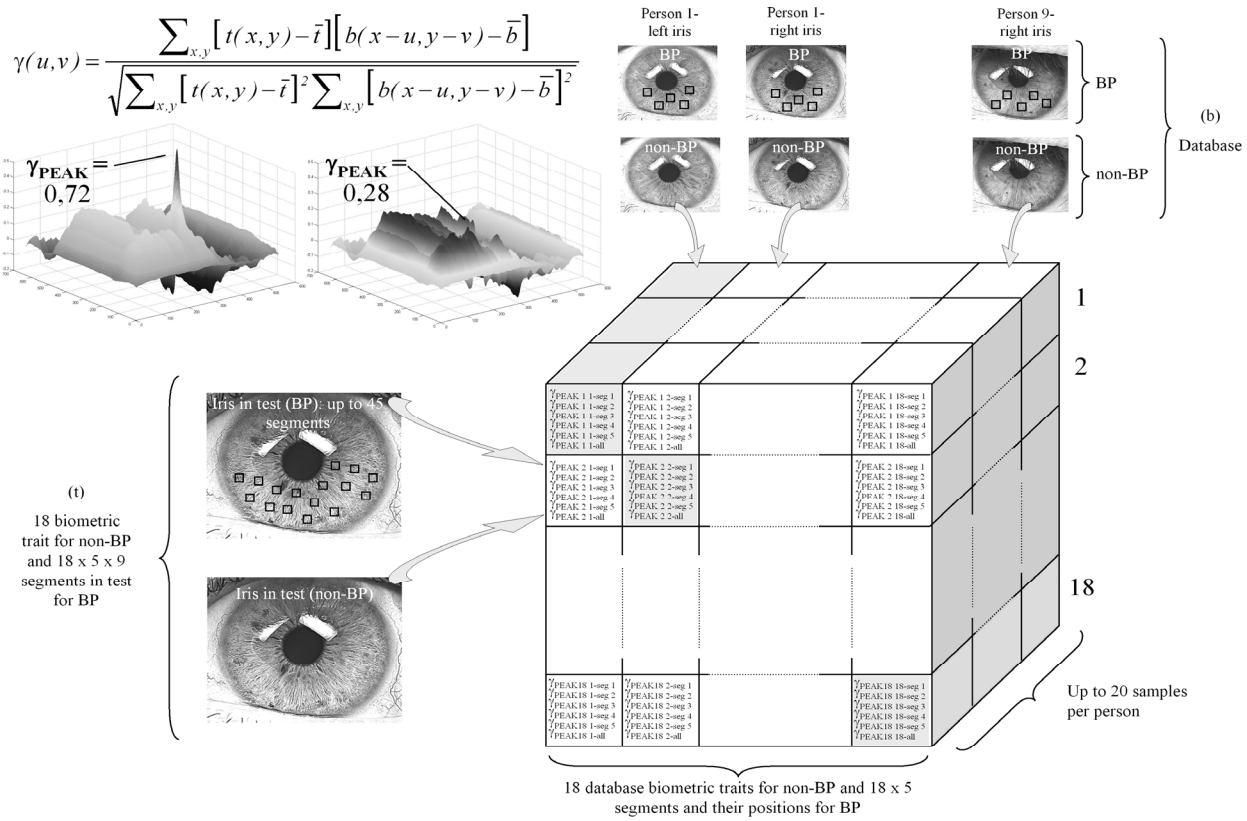

Fig. 3: Matrix of normalized cross-correlation coefficients (γ) for segments (BP) and the whole trait (non-BP). Cross-correlation curves show high peak when there is a match and a low peak for unrelated segment/whole trait. Lowest genuine γ_{PEAK} divided by the highest impostor γ_{PEAK} hints the distributions separation.

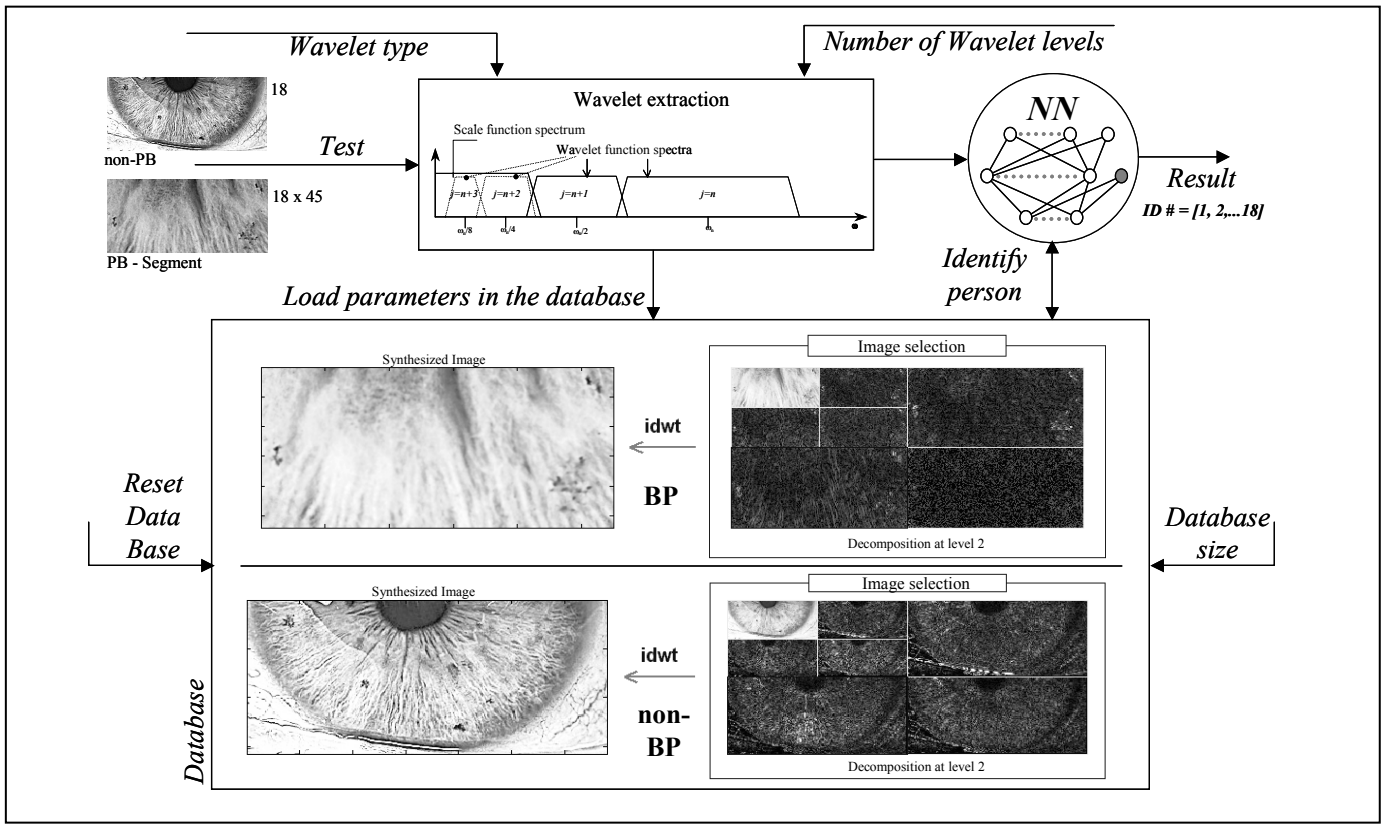

Fig. 4: Wavelet parameterization and Neural Network Classification. Implemented routine commands are displayed, e.g., wavelet type selection, database reset, etc. Test and database wavelet parameters are classified by NN. Only the ID number from 1 to 18 is output for segments (BP) or whole trait (non-BP).

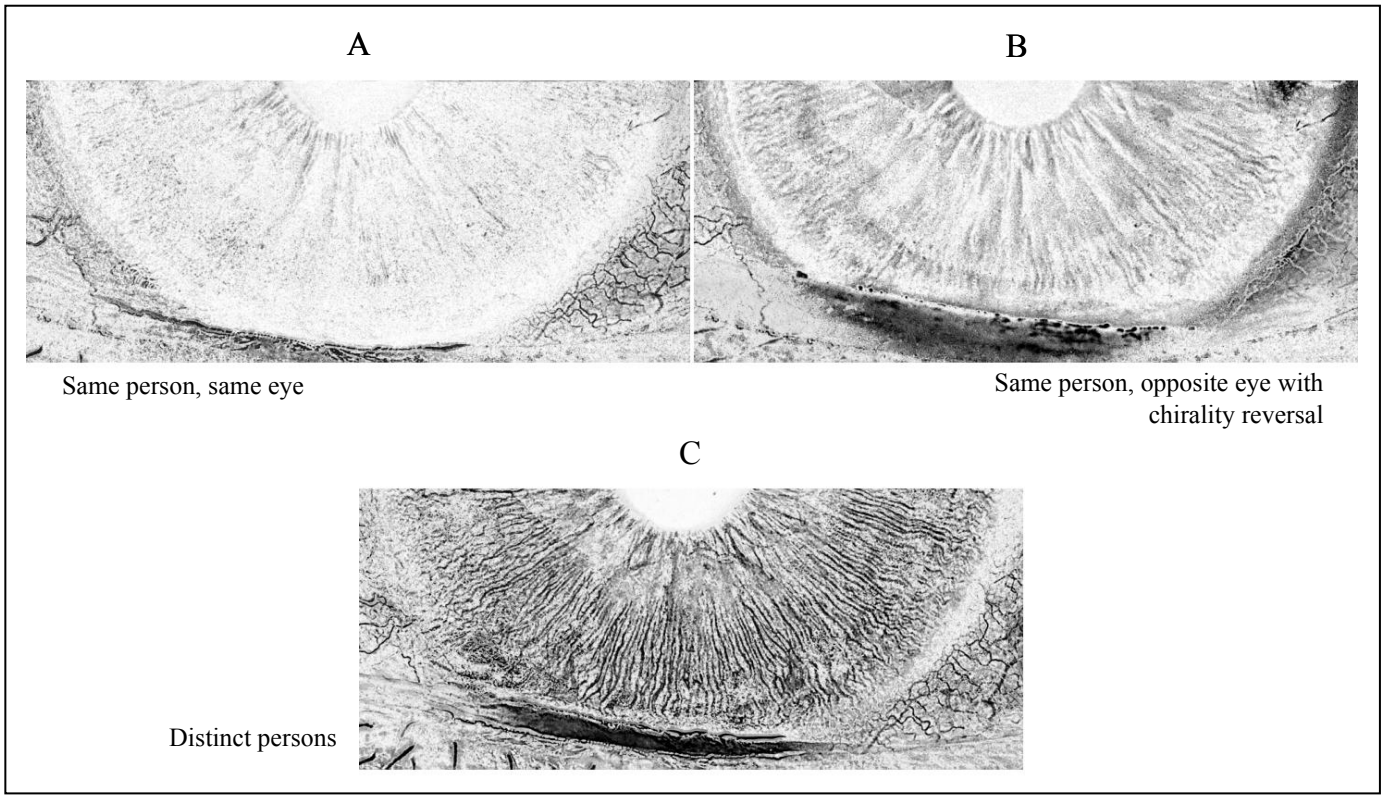

Fig. 5: Eye image difference after alignment from the population in test. “A” is the image difference of the iris samples spaced in time. “B” is the image difference of left and right iris samples captured at the same time. “C” is the iris image difference from different persons. Only the inferior eye globe hemisphere is considered. Whiter areas means low image difference, blacker areas means high difference. As expected, “A” < “B”< “C”. Wavelet + NN BP concentrates its analysis on high contrast part of the “B” image.